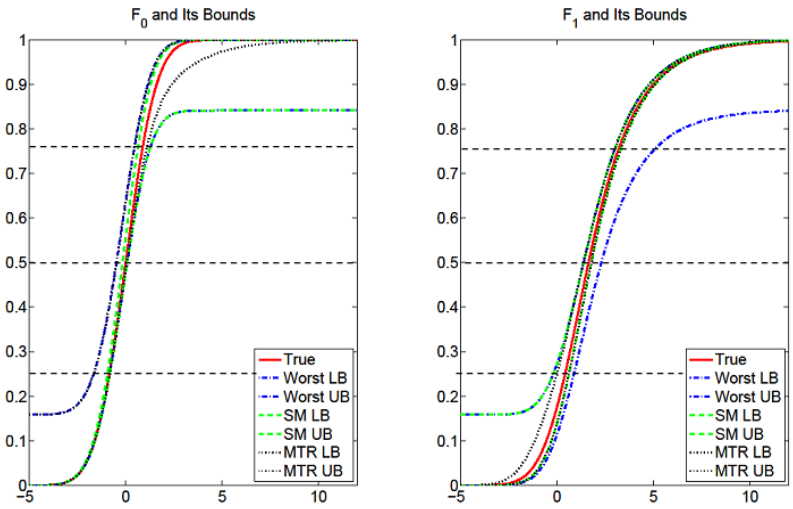

Figure 6: Bounds on the distributions of Y_0 (left) and Y_1 (right)

the lower bound on F_0 and the upper bound on F_1, respectively.

Next, I plotted bounds on marginal distributions when NSM and MTR are jointly imposed. In Figure 6, solid curves represent the true distributions of Y_0 and Y_1, and dash-dot curves and dashed curves represent their worst bounds and bounds under NSM and MTR, respectively. Figure 6 shows that if NSM and MTR are jointly considered, both upper and lower bounds improve for both F_0 and F_1 as discussed in Section 4. The quantiles of the potential outcomes can be obtained by inverting the bounds on the marginal distributions. The bounds on the quantiles of Y_0 and Y_1 are reported in Table 1

Figure 7 shows the true DTE and bounds on the DTE. Solid curve, dash-dot curves, dotted lines, dashed curves, and dashed curves with circles represent the true DTE, worst DTE bounds, bounds under NSM, bounds under MTR, and bounds under NSM and MTR, respectively. Compared to the worst bounds, the lower bound under NSM notably improves over the entire support of the DTE. Remember that the lower DTE bound improves through the upper bound on $P_0(y,1|z)$ and the lower bound on $P_1(y,0|z)$, both of which are improved by NSM, even though the DTE bounds under NSM still relies on Makarov bounds. On the other hand, although MTR directly improves the lower DTE bound from the Makarov lower bound, the improvement of the lower DTE bound by MTR is not substantial over the whole support. This is because neither the upper bound on $P_0(y,1|z)$ nor the lower bound on $P_1(y,0|z)$ improves, which are the counterfactual components